March 2024, Vol:2, Issue:1

International Journal of New Findings in Engineering, Science and Technology

journal homepage: *https://ijonfest.gedik.edu.tr/*

Dynamic simulation of the performance of a solar assisted heat pump in different climates

Bahareh Alipour[a], Maryam Karami[b*], Parisa Heidarnejad[c]

[a]*School of Mechanical Engineering, College of Engineering, University of Tehran, Tehran, Iran, e-mail:bahareh.alipour72@gmail.com*
[b]*Kharazmi University, Faculty of Engineering, Tehran,Iran, e-mail:karami@khu.ac.ir (*Corresponding Author)*
[c]*Istanbul Gedik University, Department of Mechanical Engineering, Istanbul, Turkey*

Abstract

One method to reduce energy consumption in buildings is using solar-assisted heat pumps, in which the combination of heat pump and solar collector is used to improve the thermal performance. In this paper, TRNSYS and EES software are used to simulate the performance of an indirect expansion solar-assisted heat pump. Dynamic simulation of the system is performed by changing parameters such as the mass flow rate of the collector working fluid and the collector area in five climates including Hot/Dry, Cold/Dry, Moderate/Humid, Hot/semi-Humid, and Hot/Humid. The results show that, in January, the Cold/Dry climate had the lowest free energy ratio (FER) because of the high space heating load. In this month, the Hot/semi-Humid climate has the highest FER, because of the higher solar radiation and no need for space heating. The annual FER in the Hot/Dry zone is 71% which is higher than that of other zones. The lowest FER is related to Moderate/Humid climate due to high humidity and cloudiness.

Keywords: Solar assisted heat pump; Climatic conditions; Dynamic simulation; TRNSYS.

1. INTRODUCTION

One of the methods of energy conservation is the use of solar-assisted heat pumps (SAHP) so that the temperature of the evaporator of the heat pump can be increased using solar radiation. The SAHP is made from a combination of a heat pump and solar collector, which is used as a heat source to increase the coefficient of performance (COP) [1]. In general, SAHPs are divided into two categories, direct expansion SAHP and indirect expansion SAHP based on how the solar collector and evaporator are connected [2]. In the direct expansion system, the refrigerant of the heat pump circulates directly in the solar collector, which acts as the evaporator of the system. The solar energy absorbed in the collector/evaporator is transferred to the load through the heat pump condenser. In the indirect expansion SAHP, an intermediate fluid such as water is heated in the solar system and then enters a heat exchanger for transferring to the refrigerant.

There are numerous studies on the SAHP performance in the literature. Freeman et al. [3] simulated the performance of the SAHP for providing domestic hot water (DHW) space heating (SH) of a residential building using TRNSYS software. They evaluated three modes: parallel, series and combination. The annual coefficient of performance (COP) for parallel, combined, series and conventional heat pump modes was 2, 2.5, 2.8 and 1.2, respectively. Chaturvedi and Abazeri [4] conducted their experimental study to find the steady state efficiency of a

https://doi.org/10.61150/ijonfest.2024020108

direct expansion SAHP for water heating. Test results showed that in North American winter environmental conditions, the COP for the system was between 2 and 3. The results of the study by Morrison et al. [5] showed that the annual COP of the SAHP was 1.8 to 2.3 times that of the air source heat pump (ASHP), which saved 44 to 56% of the annual energy consumption. Wang et al. [6] compared the performance of a multifunctional indirect SAHP with a domestic HP that has a solar water heater. The results showed that this pump has a better COP than the HP in terms of electrical energy consumption and efficiency. They also evaluated using four heat exchangers for integrating a heat pump air conditioner, a solar water heater and a heat pump water heater. It is found that the novel SAHP is particularly appropriate for the regions with high solar radiation. Cai et al. [7] investigated a multifunctional indirect SAHP consisting of a multifunctional HP and a solar concentrator collector. They reported that as the solar radiation increased from 0 to 800 W/m^2, the COP increased from 2.35 to 2.75. By using a suitable storage tank, Youssef et al. [8] stated that the indirect SAHP has more stability in different climates. Ma et al. [9] investigated the indirect SAHP using TRNSYS and EES in Toronto, Canada by modeling one-stage and two-stage CO_2 cycle and R410a refrigerant. The comparison of the systems showed that the performance of the two-stage cycle with a smaller compressor capacity is better than other cycles.

Ammar et al. [10] analyzed a photovoltaic/thermal (PVT)-based SAHP in terms of energy and exergy. The results show that the average COP and exergetic COP are 6.14 and 1.49, respectively. Huan et al. [11] proposed a hybrid system of solar heat pump that can work in series or parallel mode. The performance of the proposed system implemented in a university bathroom in Xi'an region. The average annual COP of the proposed system was 5.7, which is higher than the series and parallel modes, which were 3.3 and 4.3, respectively. In a study, Zhou et al [12] investigated PVT based SAHP experimentally and theoretically. The data were analyzed under typical conditions on winter days in Lüliang, China. A simulation model based on real-world conditions was developed to perform the theoretical evaluation. The comparison showed that the experimental and simulation results are in close agreement, the errors are from 4% to 9.1%, and it assures that this model is reasonable for predicting the seasonal performance of the system. The literature review, done by Lazzarin [13], showed that the heating or cooling can be supplied by the heat pump/chiller loop, in which the condenser of the heat pump increases the DHW temperature in summer or recharge the ground. Liu et al. [14] investigated a low-concentrating PVT-based SAHP to meet the electrical and thermal needs of a university building. The maximum electrical and thermal efficiency were 15.2% and 86.7%. The water-to-water heat pump works stably at a COP higher than 4 and the exergy efficiency of 73%. Meena et al. [15] optimized a solar-assisted heat pump system for water heating applications in colder climatic regions receiving least solar radiation. They found that the COP of the SAHP is about 20.1% higher using the collector with double glazing than that using the collector with single glazing. The performance assessment of PVT-based vapor injection HP indicated that the system COP is 4 in cold climate region with the solar irradiation of 500 W/m^2 [16]. Sun et al. [17] used the photovoltaic/photothermal modules in SAHP systems and reported that the power generation and photovoltaic efficiency are both improved significantly. The operational features of the combined solar-ground source heat pump system was studied and optimized by Zihao et al. [18]. The results showed that the average system COP in the winter typical month (January) for the operation of the soil source heat pump was 3.26.

The purpose of this research is to study the effect of climatic conditions on the thermal performance of an indirect expansion SAHP. The study is done numerically based on meteorological data using TRNSYS-EES co-simulator. The effect of various operating parameters such as the collector area and mass flow rate on the system performance is evaluated using the developed model.

2. SYSTEM DYNAMIC SIMULATION

In this study, the thermal performance of an indirect expansion SAHP is investigated to provide DHW and SH for a one-story house with an area of 100 m2 with 4 occupants. Figure 1 shows the schematic of the investigated system. At first, the working fluid enters into the flat plate solar collector and heated. If the temperature of the water coming out of the collector is below 20℃, the working fluid of the collector goes to the auxiliary heater to increase

the temperature, and after heating, it goes to the heat pump. If the temperature of the fluid is higher than 20℃, it will directly enter the heat pump. The working fluid inside the tank is heated by receiving heat from the heat pump condenser and then enters the auxiliary heater to reach the desired temperature (70℃). This fluid supplies DHW and SH for the case study building and then returns to the tank to be heated again by the heat coming out of the condenser and the cycle repeats.

In this study, the effect of climatic conditions on the performance of the SAHP is investigated considering five different climate zones: Hot/Dry, Cold/Dry, Moderate/Humid, Hot/semi Humid, and Hot/Humid. Five cities of Iran including Yazd, Tabriz, Rasht, Abadan, and Bandar Abbas are selected from the climate zones, respectively. Tehran, the capital of Iran, is also selected because of its importance in terms of energy consumption with more than 8.7 million populations and 3.3 million houses. The characteristics of the selected cities are listed in Table 1.

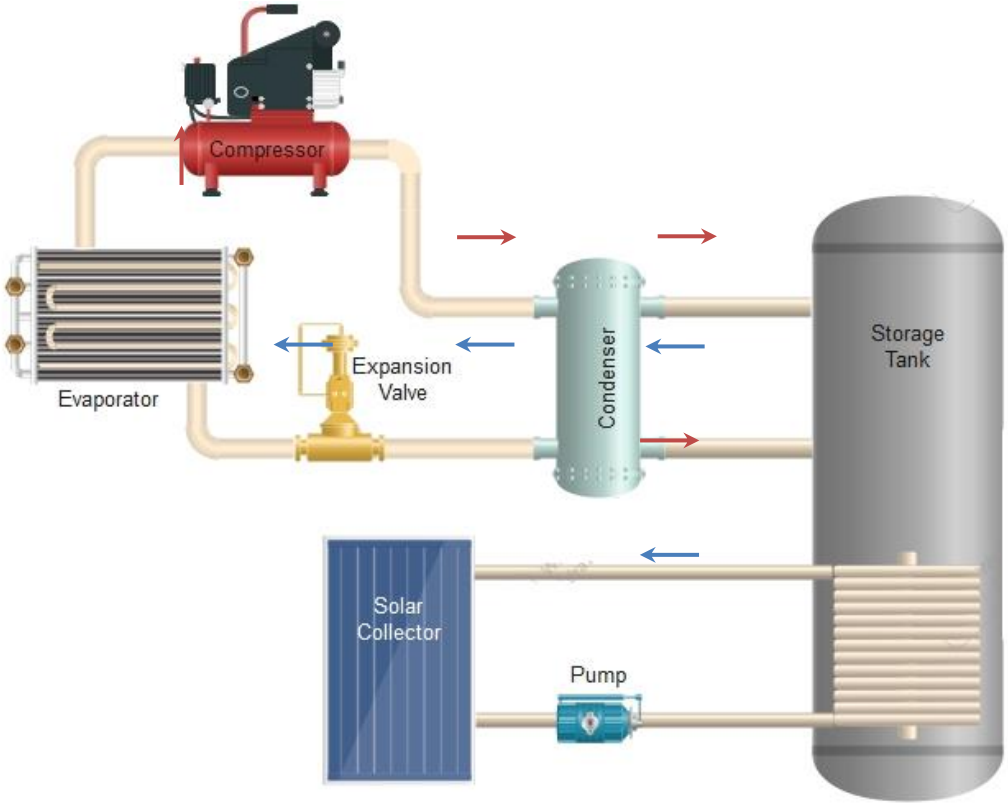

Figure 1. Schematic of the investigated SAHP

Figure 2 indicates the TRNSYS model of the SAHP. It should be noted that system controllers (Type 2b) were used to control the flow rate of the collectors and the storage tanks. For example, if the difference between the outlet and inlet temperature of the collector is less than 5℃, the collector loop pump will be turned off. Also, if the difference exceeds 10℃, the pump will turn on. Type 14b is used to simulate the daily DHW demand, of which profile is obtained in Ref. [19]. As mentioned, the cooling and heating loads of the case study building are obtained using Design Builder modeling and the results are coupled with TRNSYS using Type 9e, which calls the calculated thermal and electrical loads by linking to an external excel file.

Since TRNSYS software does not have the ability to simulate the investigated heat pump, the governing equations of the heat pump are coded in EES software and then coupled with the TRNSYS model to determine the amount of heat generated. To write the thermodynamic equations of the heat pump, the temperature and flow rate of

the inlet water are called from TRNSYS model. The refrigerant used in the heat pump is R-134a and the evaporator temperature is considered to be 10°C.

Table 1. Characteristics of the selected cities [20]

Climate (City)	Longitude (°E)	Latitude (°N)	Outdoor design dry and wet bulb temperature (℃)		Solar irradiation (kWh/m2/day)
			Winter (99%)	Summer (1%)	
Hot-Dry (Tehran)	35.41	51.19	-1.3	37.2/18.7	5.2-5.4
Hot-Dry (Yazd)	51.67	32.65	-4.9	36.9/15.8	5.2-5.4
Cold-Dry (Tabriz)	46.27	38.10	-8.5	34/16.2	3.8-4.5
Moderate-Humid (Rasht)	49.59	37.27	3	29.7/25	2.8-3.8
Hot-semi Humid (Abadan)	48.29	30.35	6	46.7/22.3	3.8-4.5
Hot-Humid (Bandar Abbas)	56.27	27.18	10.9	40.1/25.2	4.5-5.2

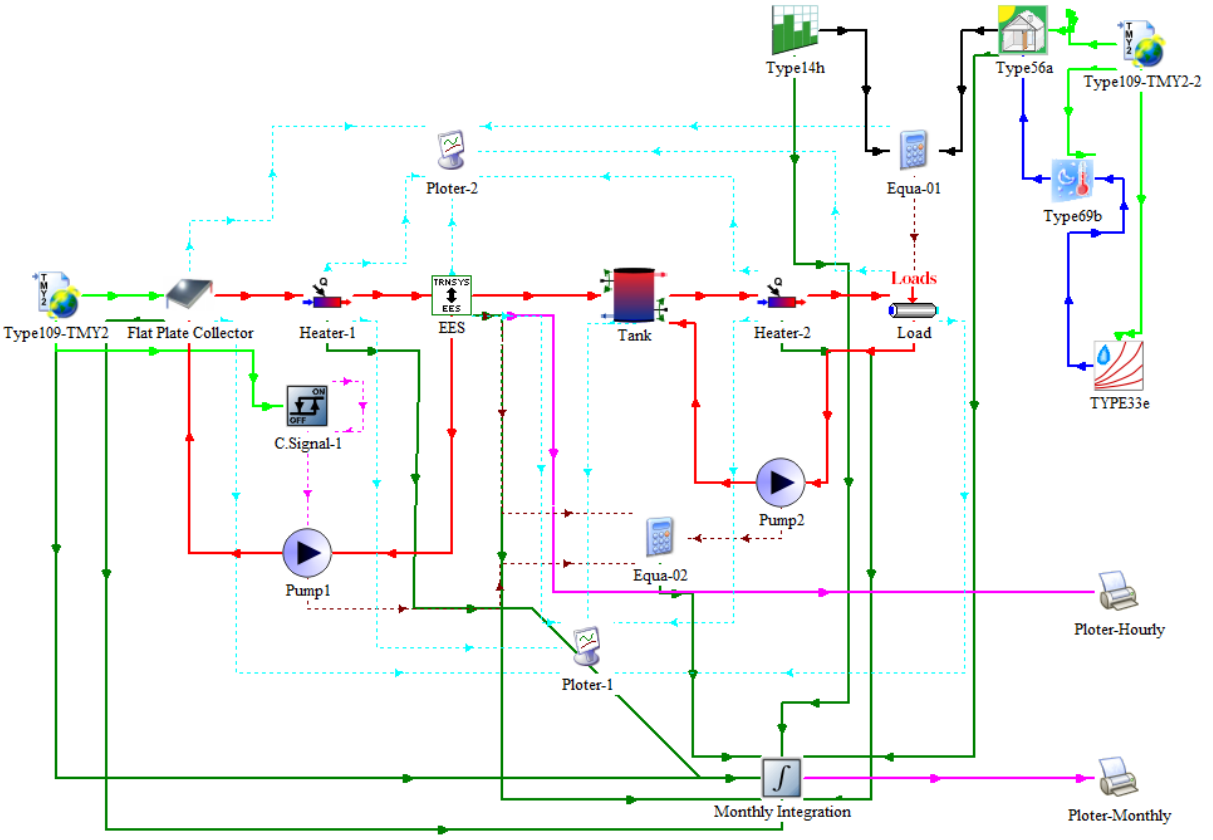

Figure 2. TRNSYS model of the SAHP

Table 2. TRNSYS types and features of the system components

Weather Data	• Type 109: Weather conditions from METEONORM and solar radiation • Type 66: Sky temperature • Type 33: Psychrometric characteristics
Water-to-water heat pump	• Type 155 (model for calling MATLAB)
Flat plate solar collectors	• Type 73 • Area: 5-20 m^2 • Mass flow rate: 36-144 kg/h • Fluid Type: Water • Maximum efficiency: 0.8
Thermal Storage Tank	• Type 4c • Thermal storage tank volume: 0.1 m^3 • Thermal storage tank loss coefficient: 2.5 $W/m^2.K$ • Internal auxiliary heater power: 2.5 kW
Circulation Pump	• Type 3b • Power coefficient: 0.5 • Maximum power: 1 kw
Auxiliary Heater 1	• Type 6 • Heater Efficiency: 0.9 • Maximum heat capacity: 100 kW • Outlet water temperature: 20℃
Auxiliary Heater 2	• Type 6 • Heater Efficiency: 0.9 • Maximum heat capacity: 100 kW • Outlet water temperature: 70℃
Cooling and Heating Load Module	• Type 9e • Type 9e is linked to an external excel file. • Type 682 is used to supply Thermal loads.
Control Signal	• Type 2d
DHW Schedule	• Type 14h
Diverter Valve and Tee Piece	• Type 11f and Type 11h

2.1. Heat Pump Modeling

Since TRNSYS software does not have the ability to simulate the investigated heat pump, the governing equations of the heat pump are coded in EES software and then coupled with the TRNSYS model to determine the amount of heat generated. To write the thermodynamic equations of the heat pump, the temperature and flow rate of the inlet water are called from TRNSYS model. The refrigerant used in the heat pump is R-134a and the evaporator temperature is considered to be 10℃.

The heat transfer in evaporator is obtained using:

$$\dot{Q}_{evaporator} = \dot{m}_R(h_{R_1} - h_{R_4}) \tag{1}$$

where h_{R_1} and h_{R_4} are the enthalpy of inlet and outlet refrigerant of evaporator and $\dot{m}_R$ is the mass flow rate of the refrigerant in the cycle.

In this study, $\varepsilon - NTU$ is used to calculate the heat exchanger effectiveness:

$$\varepsilon = \frac{\dot{Q}_{(con.evp)}}{\dot{Q}_{\max(con.evp)}} \tag{2}$$

The effectiveness of heat exchangers with phase change such as evaporators and condensers is calculated as follows:

$$\varepsilon_{hx1} = 1 - \exp(\frac{-UA}{\dot{m}_{w_1} c_{p_w}}) \quad (3)$$

where UA, $\dot{m}_{w_1}$ and c_{p_w} is the overall heat transfer coefficient, the collector fluid flow rate, and the collector fluid specific heat, respectively.

The following relations are used to calculate the heat transfer between the refrigerant and the collector working fluid in the evaporator:

$$\dot{Q}_{W_{max}} = \dot{m}_{W_1} c_{p_w} (T_{W_1} - T_{R_1}) \quad (4)$$
$$\dot{Q}_{water} = \varepsilon_{hx1} \dot{Q}_{W_{max}} \quad (5)$$
$$\dot{Q}_{water} = \dot{m}_{W_1} c_{P_w} (T_{W_1} - T_{W_2}) \quad (6)$$
$$\dot{Q}_{evaporator} = \dot{Q}_{water} \rightarrow \dot{Q}_{evaporator} = \dot{m}_R (h_{R_1} - h_{R_4}) \quad (7)$$

Where T_{W_1}, T_{w_2} , and T_{R_1} are the inlet and outlet evaporator temperatures and initial temperature of the refrigerant. The consumed work by the compressor is obtained by the following relation:

$$\dot{W}_{compressor} = \eta_c \dot{m}_R (h_{R_2} - h_{R_1}) \quad (8)$$

where η_c is the compressor efficiency.
Regarding the constant enthalpy process in the expansion valve, the heat transfer in the condenser is calculated as follows:

$$h_{R_3} = h_{R_4} \rightarrow \dot{Q}_{condensor} = \dot{m}_R (h_{R_2} - h_{R_3}) \quad (9)$$

For calculating the heat transfer from the condenser to hot water storage, the following relations are used:

$$\dot{Q}_{hotwater} = \dot{Q}_{condensor} \rightarrow \dot{Q}_{hotwater} = \varepsilon_{hx2} \dot{Q}_{hotwater_{max}} \quad (10)$$
$$\dot{Q}_{hotwater_{max}} = \dot{m}_{p_w} c_{p_w} (-T_{p_{w1}} + \frac{(T_{R_3} + T_{R_2})}{2}) \quad (11)$$
$$\dot{Q}_{hotwater} = \dot{m}_{p_w} c_{p_w} (T_{p_{w2}} - T_{p_{w1}}) \quad (12)$$

where $\dot{m}_{p_w}$, c_{p_w}, and $T_{p_{w_1}}$ are the mass flow rate to hot water storage, the specific heat of the inlet water to the tanks, and the initial water temperature in the condenser, respectively. T_{R_2} and T_{R_3} are the inlet and outlet refrigerant temperature to/from the condenser.

2.2. Performance Indicators

The COP of the heat pump is the ratio of heat transfer of the condenser to the consumed work by the compressor:

$$COP = \frac{\dot{Q}_{condensor}}{\dot{W}_{compressor}} \quad (13)$$

In this study, the free energy ratio (FER), which is the ratio of the supplied load by the solar energy to the total required load, is used to investigate the system performance:

$$FER = \frac{\dot{Q}_l - \dot{Q}_{aux} - \dot{W}_{comp} - \dot{W}_{pump}}{\dot{Q}_l} \quad (14)$$

where $\dot{Q}_l$ and $\dot{Q}_{aux}$ are the summation of DHW and SH loads and the auxiliary thermal energy supplied by the backup heater.

3. RESULTS AND DISCUSSION

In Figure 3, the monthly variation of system COP for different climates is shown. As can be seen, the maximum COP is about 3.8 and occurred in the Hot/Dry climate (Yazd) in September, because of the low SH load. In warm months, the system COP in Hot/Humid climate (Bandar Abbas) is lower than that in other climate. This is because of the high ambient humidity, which affects the incident solar radiation on the collectors. The annual average COP are 3.3, 3.4, 2.8, 2.6, 2.7, and 2.6, which are respectively obtained in Tehran, Yazd, Tabriz, Rasht, Abadan, and Bandar Abbas. It is found that in humid areas, the COP of the system is minimum, while in dry areas, the maximum COP can be obtained.

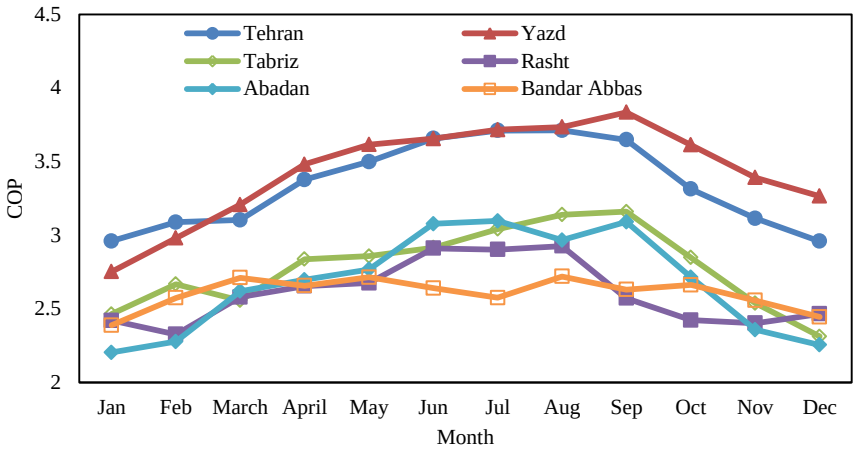

Figure 3. Monthly variation of system COP for different climates

Figure 4 shows the monthly average FER of the system in different climates. As observed from the results, the system works almost the same in the warm months in all cities except Rasht and Bandar Abbas. During this period, due to the high intensity of solar radiation, the use of auxiliary heaters is minimized. In the cold months, the cold weather causes a sharp drop in FER in Tabriz. The reason for the decrease in FER is the using an auxiliary heater in the cold months. Rasht also has the lowest annual FER, which is caused by low radiation and cloudy weather. Due to the high radiation and dry air, Yazd has the highest annual FER among the cities. Although it has a higher geographical latitude than Bandar Abbas and the radiation of Bandar Abbas is more, but it seems that the humidity and air pressure is not ineffective and the duration of cloudiness is an undeniable factor in FER. In January, Yazd has the highest FER with 61%, followed by Bandar Abbas, Abadan, Tehran, Tabriz and Rasht. In July, the FER of all cities except Bandar Abbas and Rasht is almost equal and at the maximum value. In this month, the cities of Bandar Abbas and Rasht have lower FER, which is due to the air humidity in these two cities.

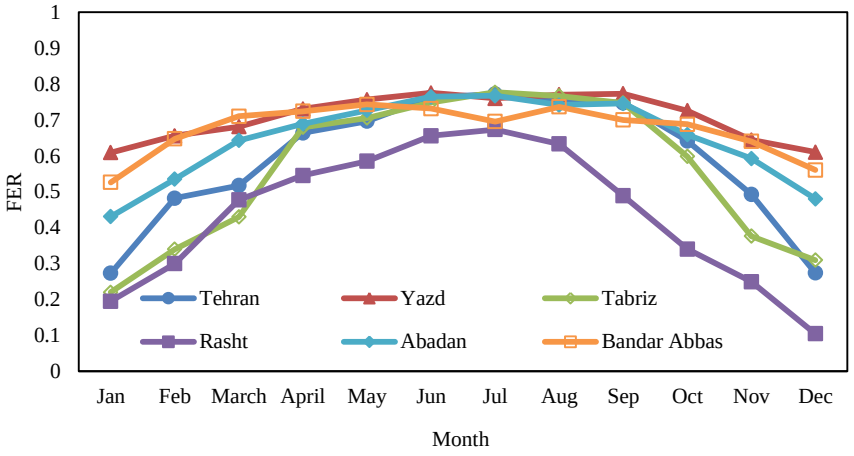

Figure 4. Monthly average FER for different climates

Figure 5 shows the annual average of FER in different climates. Yazd has the highest FER with an annual average of 70%. After that, Bandar Abbas ranks second with an average annual FER of 68% and Rasht has the lowest FER with an annual average of 44%. The reason for the big difference between Rasht and Bandar Abbas is that Rasht is a coastal city that is surrounded by the Caspian Sea on one side and the Alborz mountain range on the other. In this situation, the formation of convective clouds that stay over the city due to its proximity to the mountains makes the sky of this city cloudy in most seasons of the year. The cloud prevents the absorption of maximum radiation and on the other hand it prevents the radiation from the earth to the sky during the night. Humidity itself is one of the important factors in reducing FER. Therefore, the reduction of FER is because of cloudy weather and high humidity. On the other hand, in Bandar Abbas, which is also a coastal city, and there is the Persian Gulf on one side and dry and desert areas on the other, this causes the clouds to easily move in the direction of the wind after the formation in Bandar Abbas and the cloudiness in Bandar Abbas is much lower than in Rasht. This factor causes the air humidity to be high, but the FER rate is much higher compared to Rasht.

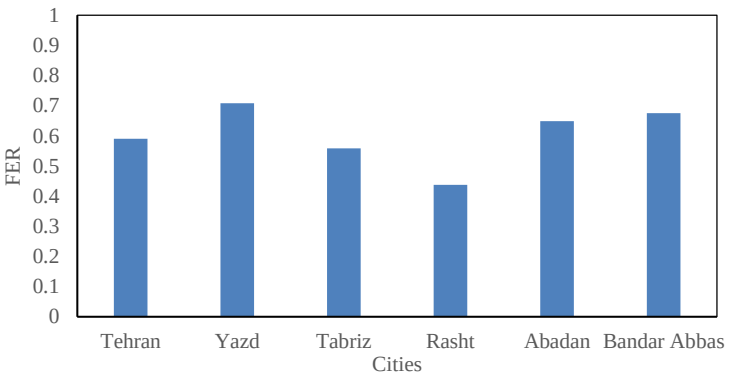

Figure 5. Annual FER for different climates

Table 3 shows the annual FER variations by the collector area in different climates. As can be seen, the largest increase in FER with the increase in the collector area is related to the Rasht by 22.41% for the increase in area from 5 m^2 to 20 m^2, which is due to the low solar radiation and cloudy weather of this city. It seems that a collector with an area of more than 15 m^2 is needed in this city. In Tabriz, with an increase in area from 5 m^2 to 10 m^2, the increase

in FER is 16.38%, and with a further increase in area, the FER increases rapidly, so it seems that the collector with an area of 10 m^2 is more suitable for this city. In other cities, FER changes are less and have almost a constant trend. On the other hand, in Bandar Abbas, there are slight changes with the increase in the collector area, which indicates that the collector area of 5 m^2 is adequate in this city.

Table 3. Annual FER increase percent with the increase of collector area

Collector area	Climate zone (City)					
	Hot/Dry (Tehran)	Hot/Dry (Yazd)	Cold/Dry (Tabriz)	Moderate/Humid (Rasht)	Hot/semi Humid (Abadan)	Hot/Humid (Bandar Abbas)
5-10 m^2	9.55	10.16	16.38	21.65	11.64	3.24
10-15 m^2	8.24	8.83	7.02	14.41	9.85	2.26
15-20 m^2	7.49	4.23	6.13	12.34	8.85	1.07

Table 4 shows the annual FER variations due to the increase in the mass flow rate of the collector working fluid in different climates. It can be concluded that the FER increases with the increase of mass flow rate. The increase in the FER with increasing the mass flow rate from 36 kg/h to 72 kg/h in Rasht is very noticeable with an approximate amount of 19% and after that the increase rate decreases. On the other hand, this trend is almost constant in other cities.

Table 4. Annual FER increase percent with the increase of collector mass flow rate

Mass flow rate	Climate zone (City)					
	Hot/Dry (Tehran)	Hot/Dry (Yazd)	Cold/Dry (Tabriz)	Moderate/Humid (Rasht)	Hot/semi Humid (Abadan)	Hot/Humid (Bandar Abbas)
36-72 kg/h	6.55	5.18	9.92	18.98	4.98	5.42
72-108 kg/h	5.48	5.95	4.08	7.52	6.41	4.10
108-144 kg/h	5.86	6.27	4.21	7.92	6.81	2.89

4. CONCLUSION

In this study, the performance of the indirect expansion SAHP using a conventional flat plate collector has been investigated in five climatic conditions. The effect of collector fluid flow rate and area were investigated using the dynamic simulation of the system by TRNSYS. The results indicated that the system in the Hot/Dry zone (Yazd) has the highest FER with an annual average of 70%. In Moderate/Humid zone (Rasht), the system has the lowest FER with an annual average of 44%. Changing the collector area improves the system performance. The average increase of COP and FER for increasing the collector area from 5 to 20 m^2 in Tehran is 38% and 23%, respectively. The COP and FER increase with the collector mass flow rate. The average increase of COP and FER in Tehran is 40% and 17%, respectively, by increasing the mass flow rate from 36 kg/h to 144 kg/h. it is concluded that considering the system performance and reducing environmental pollution, the use of SAHPs is technically and economically reasonable.

References

[1] Fu, H.D., Pei, G., Ji, J., Long, H., Zhang, T., Chow, T.T., 2012, Experimental study of a photovoltaic solar-assisted heat pump/heat pipe system, Appl. Therm. Eng.40, 343-350.
[2] Kara, O., Ulgen, K., Hepbasli, A., 2008, Exergetic assessment of direct-expansion solar-assisted heat pump systems: review and modeling, Renew. Sustain. Energy Rev.12, 1383-1401.
[3] Freeman, T. L., Mitchell, J. W., Audit, T. E., 1978, Performance of combined solar-heat pump systems, Solar Energy, 22, 125.

[4] Chaturvedi, S. K., and Shen, J. Y., 1984, Thermal performance of a direct expansion solar-assisted heat pump, Solar Energy, 33 (2), 155-162.
[5] Morrison, G. L., 1994, Simulation of Packaged Solar Heat-Pump Water Heaters, Solar Energy, 53 (3), 249-257.
[6] Wang, Q., Ren, B., Zeng, Z.Y., He, W., Liu, Y.Q., Xiangguo, X., Chen, G.M., 2014, Development of a novel indirect-expansion solar-assisted multifunctional heat pump with four heat exchangers, Building Serv. Eng. Res. Technol.0 (0), 1–13
[7] Jingyong Cai, Jie Ji, Yunyun Wang, Wenzhu Huang, 2016, Numerical simulation and experimental validation of indirect expansion solar-assisted multi-functional heat pump, Renewable Energy 93, 280-290.
[8] Youssef, W., Ge, Y., Tassou, S. A., 2017, Indirect expansion solar assisted heat pump system for hot water production with latent heat storage and applicable control strategy, 1st International Conference on Sustainable Energy and Resource Use in Food Chains, ICSEF, 180-187, Berkshire,UK.
[9] Ma, J., Fung, A. S., Brands, M., Juan, N., Moyeed, O.M.A., 2020, Performance analysis of indirect-expansion solar assisted heat pump using CO2 as refrigerant for space heating in cold climate , Solar Energy,208, 195-205.
[10] Ammar, A.A., Sopian, K., Alghoul, M.A. *et al*., 2019, Performance study on photovoltaic/thermal solar-assisted heat pump system. J Therm Anal Calorim 136, 79–87.
[11] Huan, C., Li, S., Wang, F., Liu, L., Zhao, Y., Wang, Z., Tao, P., 2019, Performance Analysis of a Combined Solar-Assisted Heat Pump Heating System in Xi'an, China. Energies, 12, *2515.*
[12] Zhou, J., Zhu, Z., Zhao, X., Yuan, Y., Fan, Y., Myers, S., 2020, Theoretical and experimental study of a novel solar indirect-expansion heat pump system employing mini channel PV/T and thermal panels, Renewable Energy 151, 674-686.
[13] R. Lazzarin, 2020, Heat pumps and solar energy: A review with some insights in the future, International Journal of Refrigeration, 116, 146-160.
[14] Liu, Y., Zhang, H., Chen, H., 2020, Experimental study of an indirect-expansion heat pump system based on solar low-concentrating photovoltaic/thermal collectors, Renewable Energy 157, 718-730.
[15] Meena, C.S., Raj, B.P., Saini, L., Agarwal, N., Ghosh, A., 2021, Performance Optimization of Solar-Assisted Heat Pump System for Water Heating Applications. Energies, 14, 3534.
[16] Yao, J., Zheng, S., Chen, D., Dai, Y., Huang, M., 2021, Performance improvement of vapor-injection heat pump system by employing PVT collector/evaporator for residential heating in cold climate region, Energy, 219, 119636.
[17] Sun, T.; Li, Z.; Gou, Y.; Guo, G.; An, Y.; Fu, Y.; Li, Q.; Zhong, X. 2024, Modeling and Simulation Analysis of Photovoltaic Photothermal Modules in Solar Heat Pump Systems. Energies 17, 1042.
[18] Zihao Qi, Yingling Cai, Yunxiang Cui, 2024. Study on optimization of winter operation characteristics of solar-ground source heat pump in Shanghai, Renewable Energy, 220, 119517.
[19] Karami, M., Javanmardi, F., 2020, Performance assessment of a solar thermal combisystem in different climate zones, Asian Journal of Civil Engineering 21:751–762.
[20] Heidarinejad, G., Delfani, S., 2007, Guidelines for the selection of outdoor design conditions for Iranian cities. Tehran: Road, Housing and Urban Development Research Center (BHRC).